Prodromal Changes in Cortical Neuron Physiology Before Amyloid Pathology in a Mild Model of Alzheimer's Disease

Katarina D. Milicevic, Ana C. Abreu, Gowri Chandran, Yan M.D. Zhu, Xiangyou Hu, Violetta O. Ivanova, Madhav Jami, Bernd Simon, Ignacio Fernández, Riqiang Yan, and Srdjan D. Antic

SUPPLEMENTAL FIGURES AND TABLES

Suppl. Fig. S1.

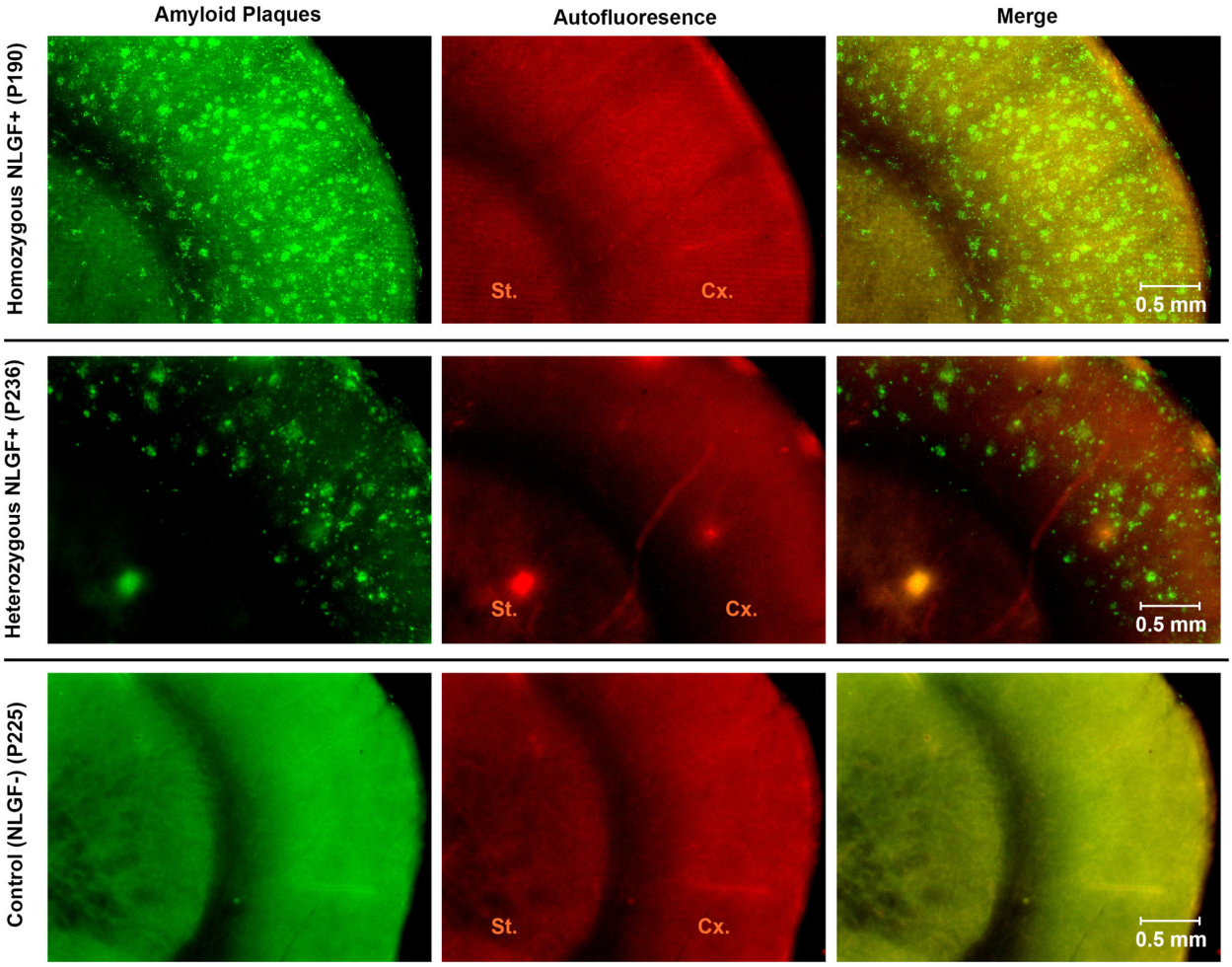

Suppl. Fig. S1. Amyloid plaques. Immunolabeling of 300 µm-thick brain sections with an anti-amyloid antibody was used to detect amyloid plaques in the cerebral cortex (Cx) and striatum (St). **Top row**: Homozygous NLGF-positive mouse at 190 days postnatal (P190). Plaques are abundant in the neocortex, with fewer detected in the striatum. **Middle row**: Heterozygous NLGF-positive mouse (AD group) at 236 days postnatal (P236). **Bottom row**: NLGF-negative mouse (CTRL group) at 225 days postnatal (P225). No plaques were detected in either cortex or striatum.

Suppl. Fig. S2.

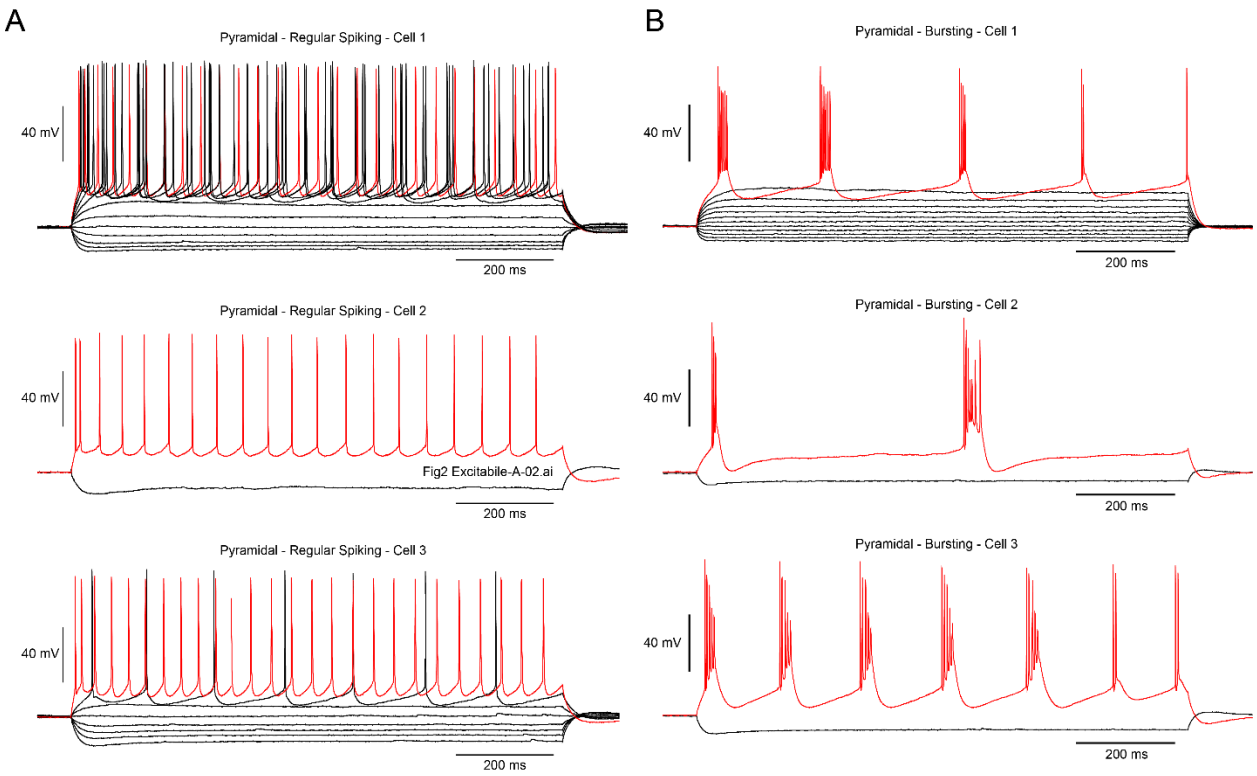

Suppl. Fig. S2. Pattern of the neuronal AP firing. (**A**) Whole cell recordings in three pyramidal cells during intracellular injections of current steps (from -200 pA, in increments of 50 pA). (**B**) Same as in *A*, except the AP spiking is not regular but rather showing a "bursting" pattern.

In this study, we define regular-spiking pyramidal neurons as cells that exhibit either (i) an initial spike doublet, or (ii) a single initial spike, followed by a train of individual action potentials, **with no additional doublets or triplets during the same current-injection step** (see panel A). Bursting pyramidal neurons, on the other hand, were identified by the presence of multiple doublets or triplets occurring during the same current-injection step (see panel B).

Suppl. Fig. S3.

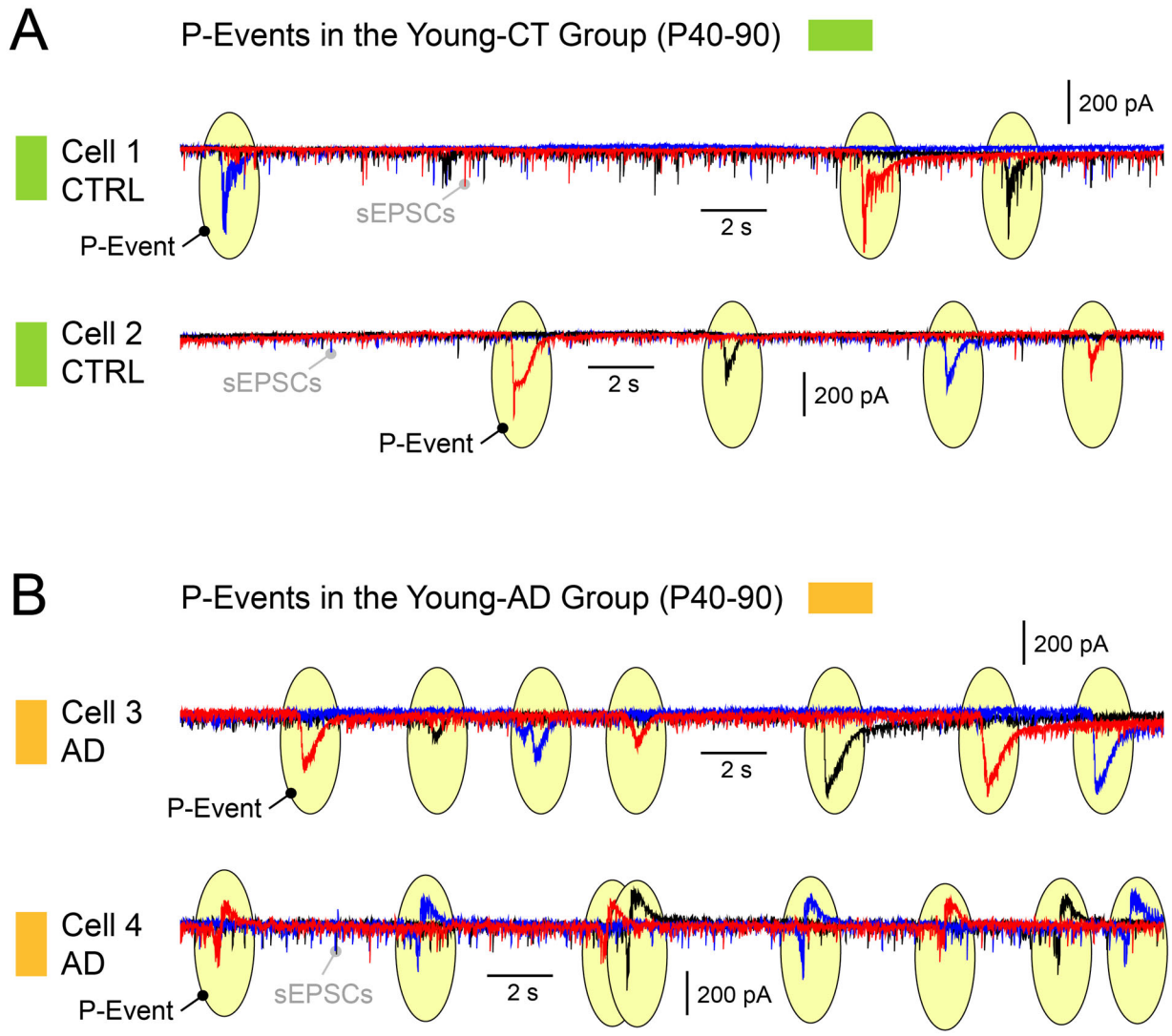

Suppl. Fig. S3. Spontaneous paroxysmal discharges in layer 5 cortical pyramidal neurons. (**A**) Voltage-clamp recordings from acute brain slices during perfusion with 4-aminopyridine (4-AP, 100 μM). Each recording session consisted of three consecutive sweeps (superimposed traces: red, black, and blue; 30 s each), yielding a total recording duration of 90 seconds per condition. Shown are recordings from two pyramidal neurons (Cell 1 and Cell 2) obtained from healthy littermate controls aged P40-P90 (Young-CT group). Yellow ellipsoids indicate paroxysmal events (P-events). Spontaneous excitatory postsynaptic currents (sEPSCs) are evident during intervals lacking P-events. (**B**) Representative recordings from two pyramidal neurons (Cell 3 and Cell 4) in brain slices from heterozygous NLGF^{+} mice P40-P90 (Young-AD group). The frequency of P-events is elevated in the AD group compared with controls (panel A).

Suppl. Table S1.

Peak assignment of metabolites identified on brains extracts by ^{1}H NMR.

Metabolite	δ_H (ppm), *J* (Hz), multiplicity
1. Leucine	0.98 (m), 0.99 (m)
2. Isoleucine	0.97 (t, *J* = 7.2 Hz), 1.03 (d, *J* = 7.0 Hz)
3. Valine	1.01 (d, *J* = 7.0 Hz), 1.06 (d, *J* = 7.0 Hz)
4. Ethanol	1.19 (t, *J* = 7.6 Hz)
5. Lactic acid	1.33 (d, *J* = 6.9 Hz), 4.05 (q, *J* = 6.9 Hz)
6. Alanine	1.48 (d, *J* = 7.2 Hz)
7. GABA	1.90 (m), 2.30 (t, *J* = 7.2 Hz), 3.01 (t, *J* = 7.2 Hz)
8. Acetic acid	1.91 (s)
9. N-acetylaspartate	2.01 (s), 2.50 (dd, *J* = 16.5; 4.2 Hz), 2.67 (dd, *J* = 16.5; 4.2 Hz)
10. Glutamate	2.04 (m), 2.14 (m), 2.39 (m)
11. Glutamine	2.11 (m), 2.45 (m)
12. Succinic acid	2.41 (s)
13. Citric acid	2.61 (d, *J* = 17.5 Hz), 2.81 (d, *J* = 17.5 Hz)
14. Aspartate	2.62 (dd, *J* = 17.5; 9.3 Hz), 2.81 (dd, *J* = 17.5; 3.6 Hz)
15. Creatine	3.05 (s), 3.90 (s)
16. Taurine	3.16 (t, *J* = 6.4 Hz), 3.33 (t, *J* = 6.4 Hz)
17. Choline	3.22 (s)
18. Phosphocholine	3.23 (s)
19. Glycerophosphocholine	3.24 (s)
20. Myo-inositol	3.24 (t, *J* = 9.5 Hz), 3.47 (dd, (*J* = 10.0, 2.8 Hz), 3.62 (m)
21. Glycine	3.49 (s)
22. Glycerol	3.55 (dd, *J* = 11.6; 6.3 Hz), 3.63 (dd, *J* = 11.6; 4.5 Hz), 3.73 (m)
23. Glucose	4.59 (d, *J* = 8.3 Hz), 5.19 (d, *J* = 3.8 Hz)
24. Inosine	4.39 (m), 4.71 (m), 6.11 (d, *J* = 6.7 Hz), 8.24 (s), 8.65 (s)
25. Adenosine	6.05 (d, *J* = 4.7 Hz), 8.20 (s), 8.32 (s)
26. Fumaric acid	6.53 (s)
27. Tyrosine	6.91 (d, *J* = 8.5 Hz), 7.18 (d, *J* = 8.5 Hz)
28. Phenylalanine	7.33 (m), 7.40 (m)
29. Histidine	7.08 (s), 7.66 (s)
30. Niacinamide	7.62 (m), 8.28 (m), 8.73 (d, *J* = 5.0, 1.6 Hz), 8.97 (d, *J* = 2.4 Hz)

Observed signal multiplicities are annotated as follows: s = singlet; d = doublet; dd = doublet of doublets; t = triplet; m = multiplet.

Suppl. Fig. S4.

1. Neurotransmission (Synaptic Transmission)

These molecules are directly involved as neurotransmitters or closely related to neurotransmitter synthesis, release, or recycling.

Glutamate – Primary excitatory neurotransmitter; **Glutamine** – Precursor for both glutamate and GABA; **GABA** – Primary inhibitory neurotransmitter; **Choline** – Precursor for acetylcholine; **Glycine** – Inhibitory neurotransmitter, mainly in spinal cord/brainstem; **Adenosine** – Neuromodulator with inhibitory effects; **Tyrosine** – Precursor for dopamine, norepinephrine, epinephrine; **Phenylalanine** – Precursor for tyrosine; **Histidine** – Precursor for histamine (a neurotransmitter); **Aspartate** – Excitatory neurotransmitter.

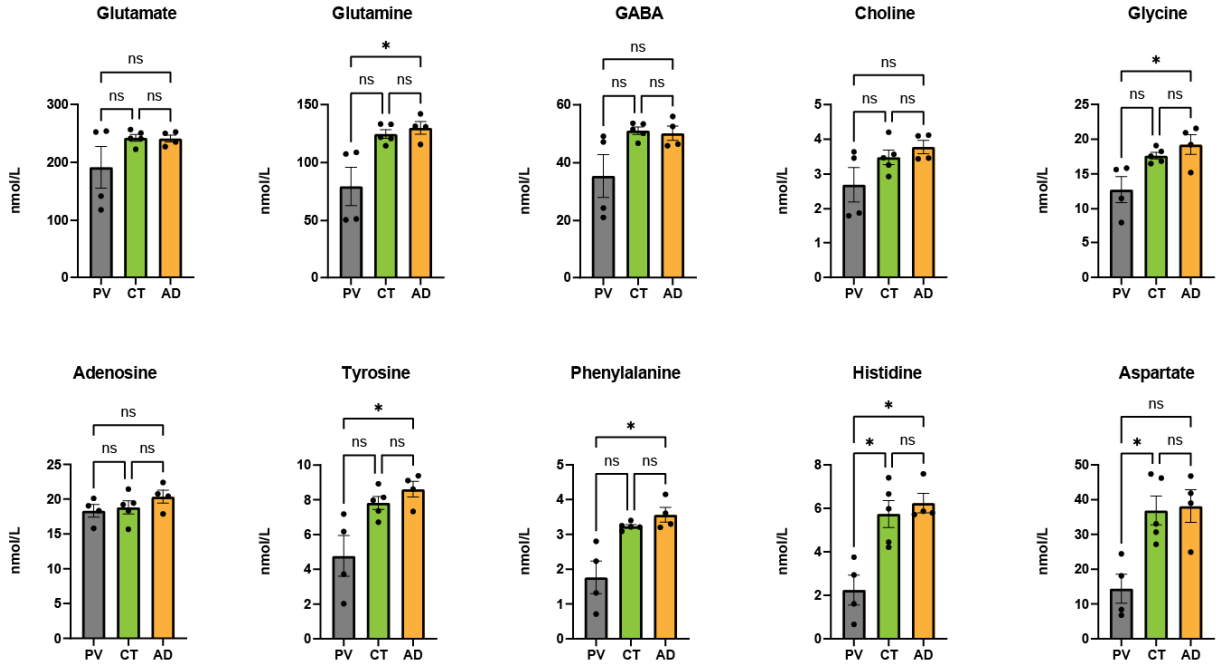

Suppl. Fig. S4. Neurotransmission. Ten molecules were classified as related to synaptic transmission. However, none showed a statistically significant difference in abundance between the Alzheimer's disease (AD) and control (CT) groups (one-way ANOVA, Kruskal–Wallis test, $p > 0.05$).

Suppl. Fig. S5.

2. Intrinsic Membrane Excitability These compounds may influence the resting membrane potential or ion gradients and thus affect neuron excitability.

Lactic acid – Alternative energy source; can influence neuronal pH and excitability; **Acetic acid** – Short-chain fatty acid, energy-related; impacts acetyl-CoA levels; **Citric acid** – indirectly affects excitability through energy metabolism (TCA cycle); **Succinic acid** – TCA cycle intermediate; **Fumaric acid** – TCA cycle intermediate; **Glucose** – Primary energy source for neurons; **Myo-inositol** – Involved in phosphatidylinositol signaling and osmotic balance; **Glycerol** – Energy metabolism and membrane lipid component; **Niacinamide** – Precursor to NAD+/NADP+; impacts oxidative metabolism and membrane function; **Creatine** – Energy buffering (ATP regeneration), important for maintaining ion pumps.

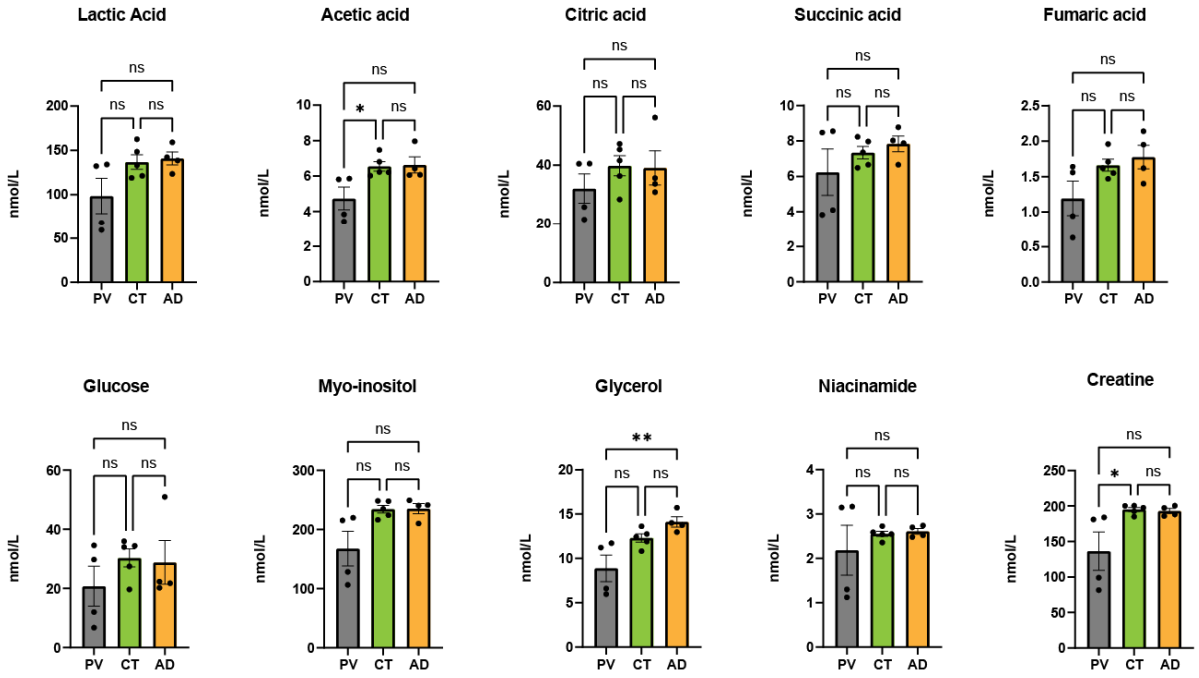

Suppl. Fig. S5. Membrane excitability. Ten molecules were classified as related to intrinsic membrane excitability. However, none showed a statistically significant difference in abundance between the Alzheimer's disease (AD) and control (CT) groups (one-way ANOVA, Kruskal–Wallis test, $p > 0.05$).

Suppl. Fig. S6.

3. Neuromodulation These molecules modulate the strength or efficacy of neurotransmission or broader neuronal/glial function.

Taurine – Osmoregulation, neuromodulatory effects, potential GABA_A agonist: **Inosine** – Neuromodulatory nucleoside, neuroprotective roles; **N-acetylaspartate (NAA)** – Marker of neuronal health; may influence osmolarity or myelination; **Glycerophosphocholine** – Osmoregulator and choline reservoir; **Phosphocholine** – Precursor in phospholipid metabolism and potential choline source; **Leucine** – Modulates neurotransmission and protein synthesis pathways; **Isoleucine** – BCAA; similar modulatory roles; **Valine** – BCAA; similar modulatory roles; **Alanine** – Involved in amino acid metabolism; minor neuromodulatory effects; **Ethanol** – Potent neuromodulator affecting multiple receptor systems.

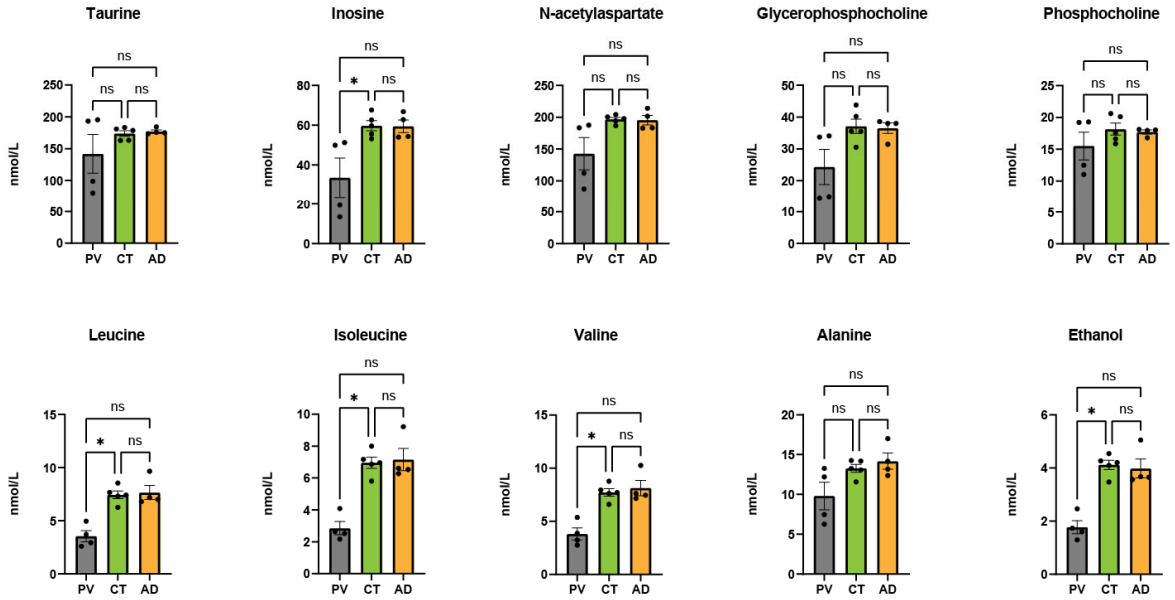

Suppl. Fig. S6. Neuromodulation. Neuromodulation is the process by which certain substances or signals regulate the activity of neurons, changing how neurons respond to other inputs. Neuromodulation typically adjusts the overall tone or excitability of neural circuits rather than triggering direct responses like traditional synaptic transmission. Ten molecules were classified as related to neuromodulation. However, none showed a statistically significant difference in abundance between the Alzheimer's disease (AD) and control (CT) groups (one-way ANOVA, Kruskal–Wallis test, $p > 0.05$).

Suppl. Fig. S7. Supervised Approach PCA

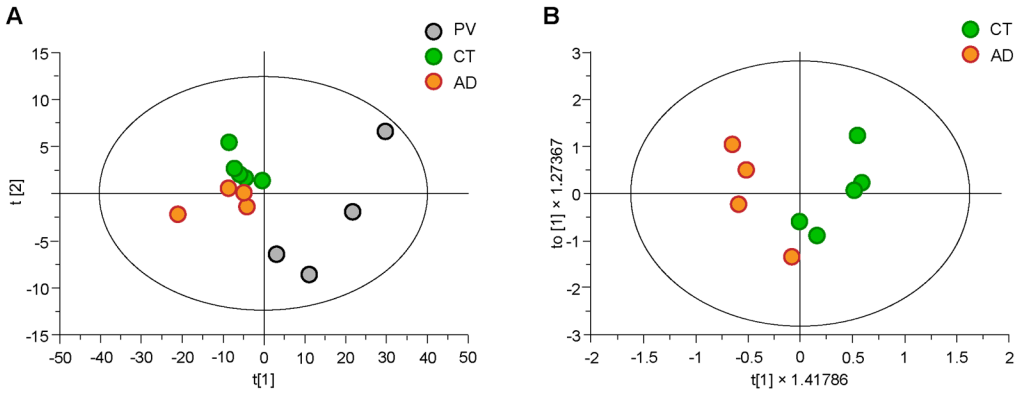

Suppl. Fig. S7. Supervised multivariate analysis of ^{1}H NMR spectroscopy data. (A) Partial Least Squares Discriminant Analysis (PLS-DA) model based on group labels (CT: control, AD: Alzheimer's disease, PV: presymptomatic vehicle) aimed at maximizing group separation. **(B)** Orthogonal Partial Least Squares Discriminant Analysis (OPLS-DA) model comparing CT and AD groups to enhance discrimination by removing orthogonal variation unrelated to class separation. In both cases, the dataset (n = 12 mouse brains) yielded low predictive performance (Q^2 < 0.3) and lacked statistical significance (*p* (cv-ANOVA) > 0.05), suggesting that the observed clustering lacks statistical significance and should be interpreted with caution.

Suppl. Fig. S8.

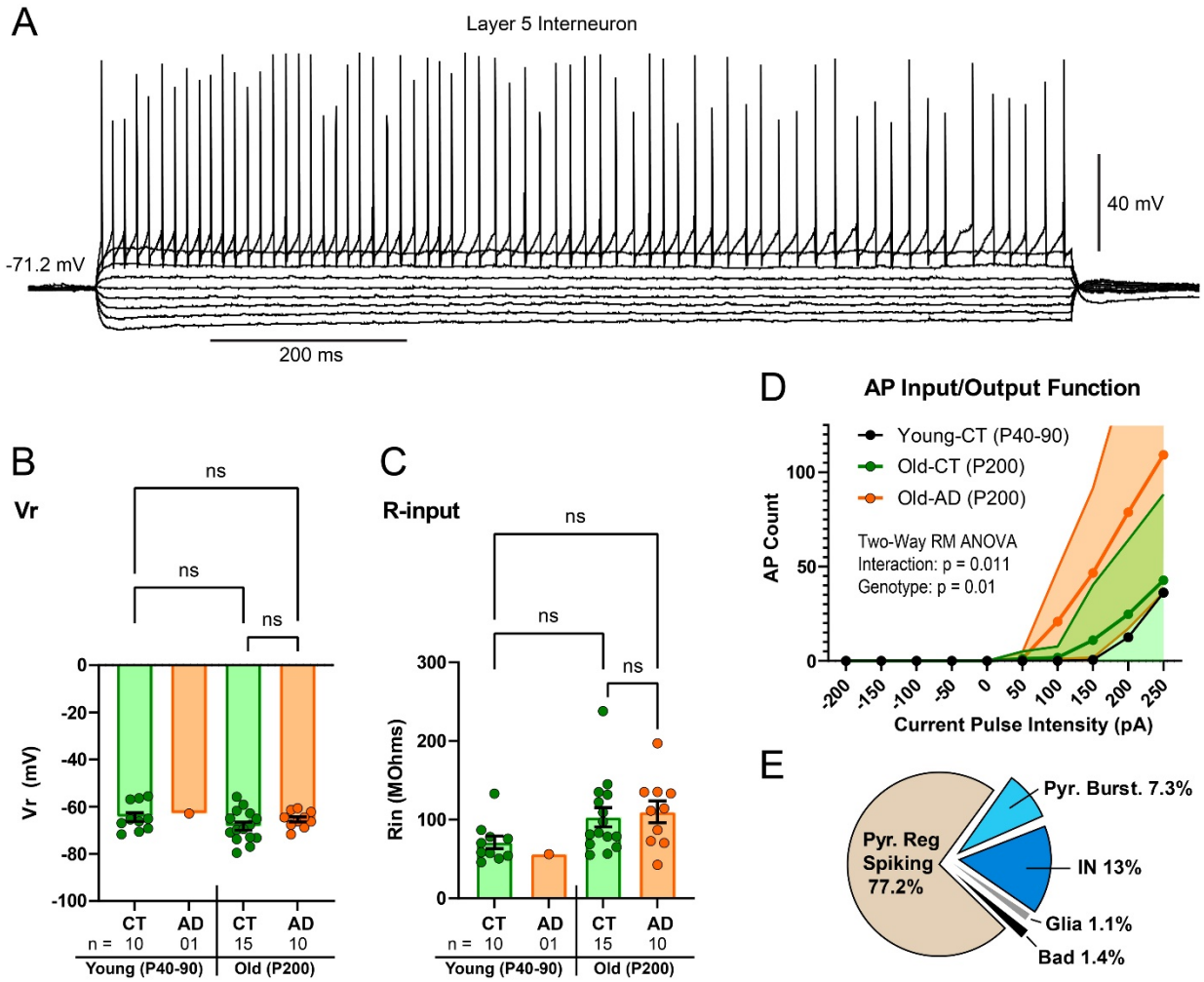

Suppl. Fig. S8. Increased AP firing in cortical interneurons in the presence of AD pathology. (**A**) Representative current-evoked voltage responses from a putative fast-spiking interneuron (IN). (**B**) Average resting membrane potential (Vr) across experimental groups (bars) and individual cells (circles). One-way ANOVA; post hoc Tukey's test, no significant group differences ($p > 0.05$). The Young-AD group had only one recorded cell (n=1), and was therefore excluded from post hoc comparisons. (**C**) Average input resistance (Rin) across groups (bars) and individual cells (circles). One-way ANOVA; Sidak post hoc test, no significant group differences ($p > 0.05$). (**D**) Action potential (AP) firing rates in response to increasing current injections. The AD group (NLGF-positive; orange) showed significantly elevated firing compared to age-matched NLGF-negative controls (green) (two-way repeated-measures ANOVA). A third group (black) includes young NLGF-negative controls (P40–90). The fourth group, Young-AD group, had only one recorded cell (n=1) and is therefore not shown. (**E**) Cell type composition in the dataset (n=276 patched cells): Regular-spiking pyramidal neurons comprised 77.17 % (n=213), AP-bursting pyramidal neurons 7.25 % (n=20), putative interneurons 13.04 % (n=36), glial cells 1.09 % (n=3), and recordings deemed poor quality, "Bad", 1.45 % (n=4).